# Coincidence technique using synchrotron radiation for triple photoionization: Results on rare gas atoms

J. H. D. Eland,[1] P. Linusson,[2] L. Hedin,[3] E. Andersson,[3] J.-E. Rubensson,[3] and R. Feifel[3]
[1]*Physical and Theoretical Chemistry Laboratory, Oxford University, South Parks Road, Oxford OX1 3QZ, United Kingdom*
[2]*Department of Physics, Stockholm University, AlbaNova University Centre, SE-106 91 Stockholm, Sweden*
[3]*Department of Physics and Material Sciences, Uppsala University, Box 530, SE-751 21 Uppsala, Sweden*
(Received 28 September 2008; published 29 December 2008)

Final-state trication spectra and electron distributions produced by soft x-ray single-photon triple ionization of rare gas atoms have been obtained by a multiple-coincidence technique using storage-ring synchrotron radiation. The technique uses electron time of flight with ion detection to overcome the problem of high repetition rates in single-bunch operation. A correction needed to the triple-ionization energy of Kr currently listed in standard tables is confirmed, and the method's ability to examine the three-electron distributions, characterizing the ionization mechanisms and post-collision interactions, is illustrated.

DOI: 10.1103/PhysRevA.78.063423 PACS number(s): 32.80.Fb, 32.80.Zb, 34.50.Gb

## I. INTRODUCTION

Multiple-ionization processes are increasingly recognized as important in the interstellar medium, in cometary halos, and in planetary atmospheres. Over the years, significant understanding of single-photon double-ionization processes has been obtained both experimentally and theoretically [1,2]. In contrast, triple photoionization has hardly been studied at all as yet. A few works focused on the investigation of the total triple-ionization cross section of Li, for which good agreement has been found between theory [3–6] and experiment [7,8]. Differential cross sections of three escaping electrons have been considered theoretically, too, in particular with respect to selection rules for different electron-momentum configurations [9], with respect to angular correlations [10–12] and with respect to energy correlations [13,14]. Recently, some experimental information on the angular and energy distributions of triple ionization has been obtained by studying double Auger transitions in rare gas atoms [15–17]. Very recently, the first experimental study of electron correlations in valence triple ionization of Ar has been reported by Hikosaka *et al.* [18], which gave the first insights into detailed energy distributions. As this work shows, not only direct, but also indirect triple-ionization routes are important, which challenges existing theoretical work for further development.

In general, triple photoionization offers interesting new scenarios for interactions and energy exchange between several charged particles. In the case of triply ionized atoms, as studied in the present work for the rare gases, one deals with a four-body Coulomb problem [10,11]. This field is still quite unexplored, which is most likely related to the rareness of proper experimental tools needed for such investigations.

This paper reports an experimental technique based on a magnetic bottle [19], which enables detailed studies of triple ionization by soft x-ray single photons produced as synchrotron radiation from electron storage rings. Whereas many recent results on double photoionization could be obtained in small-scale laboratories (see, e.g., [20–28] and references therein), this has not been possible for triple ionization since no suitable light sources yet exist in the necessary energy region above 50 eV photon energy. (High harmonic generation using femtosecond lasers offers the prospect of such a source [29,30], but no practical device is available yet for this purpose.) Synchrotron radiation has ample energy and intensity, but has a drawback which mitigates against its use with the most effective modern tool for multi-ionization coincidence spectroscopy, the magnetic bottle time-of-flight (TOF) technique [20]. The problem is that even in single-bunch mode at large ring facilities, the time between light pulses is shorter than the electron flight time for all but very-high-energy electrons or over a very short path length. When an electron is detected, there is ambiguity regarding the identity of the light pulse which produced it (from among a number of pulses which preceded its detection).

The first method to overcome this difficulty was to select a photon energy at which an electron of known energy is emitted in creating an inner-shell vacancy [16]. Subsequent electrons emitted in single, double, or triple Auger effects can then all be referenced to this first photoelectron [31]. This method is excellent for the limited range of processes to which it applies. Uncertainties can be reduced in cases where the ionization energies are known by applying energy conservation, but ambiguities still remain. Most recently, a fast chopper which selects individual light pulses at a usable repetition rate has been developed and applied to the triple ionization of Ar [18]. This is indeed a very powerful and generally applicable technique, with only the slight disadvantage that it reduces the rate at which data can be gathered.

In this paper we propose and demonstrate a method in which the simultaneously created ions are detected in coincidence with the electrons. The ion flight times are known and unambiguously identify the ionizing light pulses. Besides removing the energy uncertainty, this technique very strongly suppresses the background of false coincident electron pairs, which is prominent in most spectra measured with electrons alone. We present directly measured valence triple-photoionization spectra of Ne, Ar, and Kr—that is, triple ionization not involving inner-shell holes and Auger processes. The electron distributions in this valence triple photoionization (TPI) are shown to exhibit characteristics of separable direct and indirect mechanisms. The distributions attributed

 

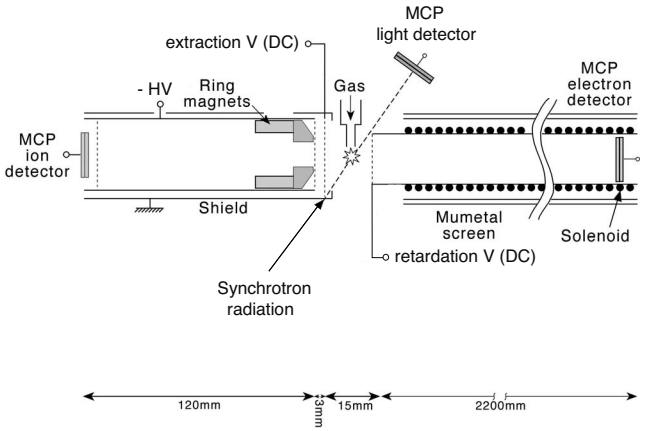


FIG. 1. Scheme of the experimental setup.

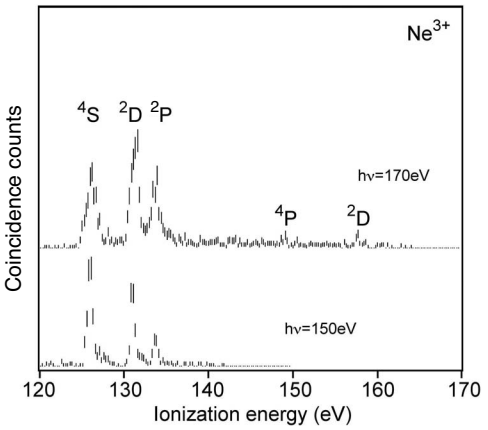


FIG. 2. Triple-Photoionization spectra of Ne at 150 eV and 170 eV photon energy. The three low-energy states $^4S$, $^2D$, and $^2P$ all arise from the valence configuration $3s^2 3p^3$, while the two higher states $^4P$ and $^2D$, barely visible at 170 eV, come from $3s^3 p^4$. The error bars represent two standard deviations, from the counting statistics.

to direct TPI can be compared with the only existant predicted distributions, which have been calculated for the case of Li (see Refs. [13,14]).

## II. EXPERIMENTAL DETAILS

Experiments were conducted at the U49/2-PGM2 [32] beamline at BESSY-II, Berlin, where the time between light pulses in single-bunch mode is 800.5 ns [33]. The well-collimated light beam and the effusive jet of target gas which it intersected were both aligned perpendicular to the axis of the collinear ion and electron TOF spectrometers as schematically shown in Fig. 1. The end field of the magnetic bottle electron TOF spectrometer was provided by a set of four hollow ring magnets and a soft iron pole piece, through which ions could pass on their way to a field-free flight path and detector. The setup was similar to the one developed for laboratory use with a pulsed discharge lamp light source [34], with the essential difference that the electron flight tube was insulated from the exterior vacuum vessel and could be polarized to accelerate or decelerate the electrons. The electron, ion, and ring pulse (time reference) signals were recorded using a multichannel, multihit time-to-digital converter, whose clock was started by the first electron to arrive from each observed event.

In order to extract photoions, a weak continuous drawout field (7 V $cm^{-1}$) was applied in the ionization region; ions were accelerated further by an adjustable potential after passing through a first grid. The acceleration was adjusted for each target atom to allow the ion of interest to be distinguished from all others, modulo the pulse repetition period of 800.5 ns. The individual mass peaks were narrow enough to make this distinction possible for undissociated atomic ions, because of tight collimation (ca. 100 $\mu$m) of the ionizing light beam and a low effective kinetic temperature of the ions. With the narrow light beam, time focusing was not necessary. A low transverse kinetic temperature of the ions was ensured by placing the orifice of the target gas jet several mm from intersection with the light beam so that only atoms with trajectories almost perpendicular to the spectrometer axis were ionized.

The field that extracts ions from the source also accelerates the photoelectrons in the opposite direction, increasing their energy by about 7.5 eV. This increase in electron energy would seriously diminish the resolution for low-energy electrons if it were not compensated for by application of a 7-V retarding potential to the ion flight tube. One effect of the drawout and retarding fields was to reduce the electron energy resolution for low-energy electrons to about 150 meV. For higher energies the peak widths follow a numerical resolution $E/\Delta E$ of about 30. A second effect was to complicate the relationship between TOF and electron energy; the usual simple three-parameter formula [20] had to be replaced by an algorithm in which acceleration, deceleration, and free-flight times are individually accounted for. Calibration was based on measurements of the photoelectron lines from $3d$ ionization of Kr, with allowance for known post-collision interaction (PCI) effects. Ancillary measurements were made without ion coincidences and using a conical permanent end magnet, with which resolution is better [34], to check the calibration. The sample gases were of commercial standard with stated purities of better than 99.9%.

Because the cross sections for triple photoionization are very small and because the present experiment is a quadruple-coincidence experiment, where three electrons and an ion are detected simultaneously, the useful count rates are low and the statistics of the present data are limited. Total count rates, dominated by abundant single and double ionization, must be limited to avoid excessive false coincidence counting. Each of the data sets presented here required a runtime of about 1 h. Future experiments with improved equipment and longer runs will improve the resolution and statistics, but to a certain extent only.

## III. RESULTS AND DISCUSSION

Triple-ionization spectra of Ne at 150 eV and 170 eV photon energy, Ar at 100 eV and 120 eV, and Kr at 90 eV are shown in Figs. 2–4. All these photon energies are below

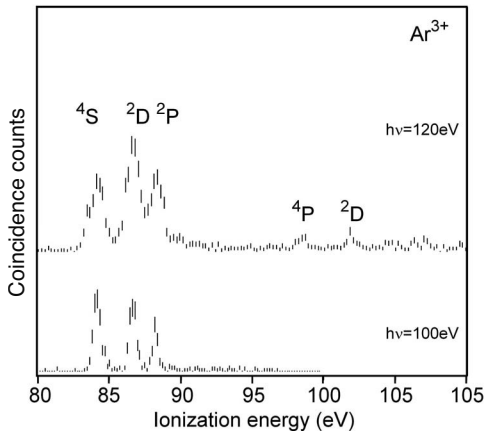


FIG. 3. Triple-photoionization spectra of Ar at 100 eV and 120 eV photon energy, akin to Fig. 2.

the onset of any inner shells or near-edge structures. Because the spectra have been measured in coincidence with the triply charged ions, eliminating timing uncertainty, and because the magnetic bottle gathers essentially all electrons, they give complete relative intensities of the resolved states. The terms visible in all the spectra are $^4S$, $^2D$, and $^2P$ from $3s^23p^3$; spin-orbit splitting is resolved only for Kr. Their relative intensities are collected in Table I and are compared with the statistical weights. A common theme is that the intensity ratio $[^2D]/[^2P]$ approaches the statistical limit as photon energy increases, while the intensity seen for $^4S$ tends to be higher than statistical relative to the other states for the lower photon energies. The terms $^4P$ and $^2D$ from the $3s3p^4$ configuration are weakly populated at the higher energies.

In the case of Kr, the lowest level of the $Kr^{3+}$ ion is located experimentally at $74.03 \pm 0.05$ eV relative to the neutral atom. This ionization energy is lower than the value given in standard tables (75.31 eV [35]) by 1.28 eV. This huge discrepancy has been noted before [37] and is attributed

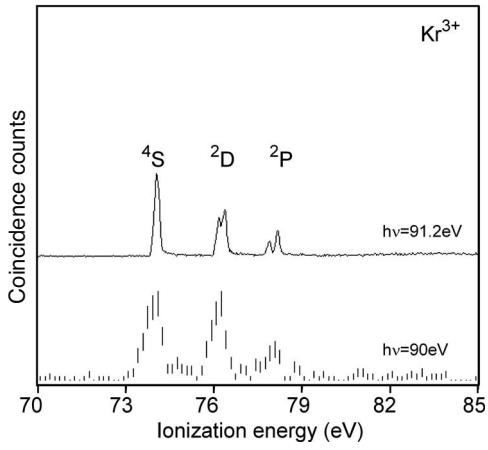


FIG. 4. Triple photoionization of Kr at 90 eV photon energy (lower data set, with error bars). The upper curve at 91.2 eV, on the $p^*$ resonance, is included to demonstrate the better resolution obtainable in this case from runs without ion coincidences. The experimentally determined lowest triple-ionization energy is $74.03 \pm 0.05$ eV.

nonspecifically to incorrect identification of Rydberg states used for extrapolation to the older value. For the lighter elements there is good agreement between the present and standard [35] energies.

The relative populations of final triply ionized states are certainly related to the mechanisms involved in their formation, which are likely to be revealed by the electron energy distributions. Because three electrons share excess energy in the formation of each final state ($h\nu$-TIP) (TIP=triple ionization potential), the distributions must be represented as a two-parameter plot. For the first electron detected, which has the highest energy, the minimum possible energy is one-third of the available excess; the maximum is equal to the whole excess. For the second detected electron the minimum energy is zero and the maximum is one-half the excess, while for the third electron the minimum is zero and the maximum is one-third of the total excess. Since each ionization event necessarily produces one each of all three electrons, an unbiased representation (in the sense that a completely random distribution would give an even distribution of intensity) is produced by plotting intensity (color or grayscale) against $2E_2$ and $3E_3$. The energy $E_1$ can be deduced at each point as $h\nu$-TIP-$(E_2+E_3)$. Samples of the resulting triangular plots are shown in Figs. 5 and 6.

The electron–triple-distribution plots have several common features. In the plots for $Rg^{3+}$ ($^4S$) formation, there is an area of enhanced intensity at the left (low $E_3$) extending precisely up to the energy of $^2D$ above $^4S$. In some data a weaker range of enhanced intensity up to the energy of $^2P$ can be discerned, but at higher $E_3$ the intensity is low and uniform, independent from $E_2$. In the formation of $Rg^{3+}$ ($^2D$) a similar pattern is seen, with enhanced intensity up to the energy difference between $^2P$ and $^2D$. In $^2P$ formation the intensity is uniformly distributed, as far as can be judged from these preliminary data. The interpretation of the patterns is clearly that one pathway to rare gas triple ionization involves Rydberg states of intermediate $Rg^{2+}$ dications, belonging to series converging on the higher $Rg^{3+}$ states. This is closely akin to the well-studied process sometimes called valence multiplet decay (VMD) in double ionization. With the exception of one strong resonance at 2.16 eV electron energy in the formation of $Ar^{3+}$ ($^4S$), the individual autoionizing states are not resolved under the present conditions and may not be resolvable if their lifetimes are short. In formation of the final $^4S$ states there is a noticeable accumulation of intensity at the lowest values of $E_2$. This shows that in the formation of the intermediate dication states the electron pair distributions are hollow or U-shaped, favoring one high-energy and one low-energy electron.

It is no great surprise that triple photoionization, like double photoionization, has a large contribution from indirect processes. Three-electron emission can in principle involve intermediate singly charged as well as doubly charged states, as indeed happens in the double Auger effect [16]. We have no clear evidence for such a process in valence triple photoionization. The involvement of both a singly and a doubly charged intermediate state would reveal itself as a sharp spot of intensity, rather than a line or area, in distributions such as in Fig. 5.

The available theoretical treatment of triple ionization is almost entirely limited to discussion of the especially inter-

TABLE I. Energies and relative intensities $I$ (peak areas) of $Rg^{3+}$ final states.

| State | Energy (eV) Present | Energy (eV) NIST, Moore [35,36] | $I$ (150 eV) | $I$ (170 eV) | $I$ (statistical) |
|---|---|---|---|---|---|
| | | **Neon** | | | |
| $^4S$ | 125.99 | 126.07 | 149 | 85 | 40 |
| $^2D$ | 131.05 | 131.51 | 100 | 100 | 100 |
| $^2P$ | 133.75 | 134.13 | 40 | 64 | 60 |
| State | Energy (eV) Present | Energy (eV) NIST, Moore [35,36] | $I$ (100 eV) | $I$ (120 eV) | $I$ (statistical) |
| | | **Argon** | | | |
| $^4S$ | 84.05 | 84.30 | 113 | 75 | 40 |
| $^2D$ | 86.67 | 86.92 | 100 | 100 | 100 |
| $^2P$ | 88.33 | 88.63 | 48 | 69 | 60 |
| State | Energy (eV) Present | Energy (eV) NIST[35] | $I$ (90 eV) | | $I$ (statistical) |
| | | **Krypton** | | | |
| $^4S$ | 74.03 | 75.31 | 122 | | 40 |
| $^2D_{3/2}$ | 76.12 | 77.42 | 100 | | 100 |
| $^2D_{5/2}$ | 76.36 | 77.62 | 100 | | 100 |
| $^2P_{1/2}$ | 77.85 | 79.16 | 31 | | 60 |
| $^2P_{3/2}$ | 78.15 | 79.45 | 31 | | 60 |

esting direct process [13,14]. By analogy with double ionization we can reasonably suppose that two contributors to the direct process will be double shake-off and double knock-out. Shake-off is expected to dominate at high excess photon energy and to give one fast electron and two slower ones. Knock-out should give a more equal division of energy among the three electrons and play a larger part nearer to threshold. If these processes produce final states with population probabilities which vary substantially with photon energy, it should be possible to reveal their relative importance in the triple ionization by studying the relative intensities of the spectral lines at various photon energies. Possibly, the

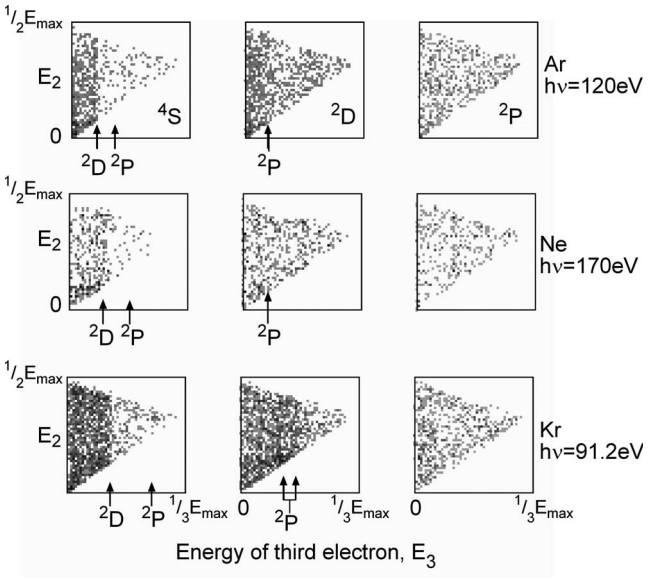


FIG. 5. Electron–triple-energy distributions in photoionization of Ar at 120 eV, Ne at 170 eV, and Kr at 91.2 eV for the formation of the separate final states, measured in coincidence with the triply charged ions. All nine plots are on the same reduced scales, as explained in the text. Vertical arrows mark the energies of higher trication states above the one being formed. The Kr data, taken on a pre-edge resonance, are included for the sake of better statistics.

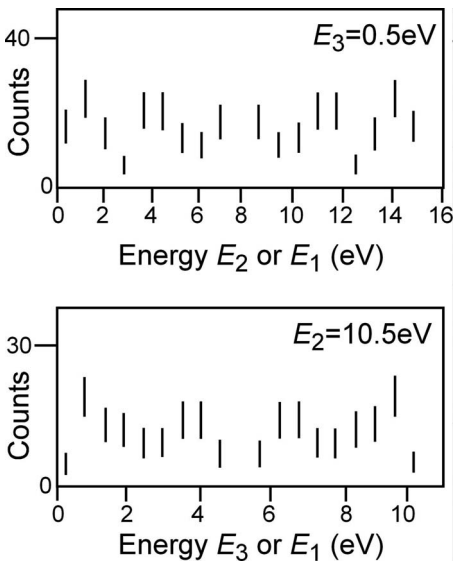


FIG. 6. Two cuts of the electron–triple-energy distribution in formation of $Ar^{3+}$ ($^2P$) at 120 eV photon energy. The central gap is caused by detector dead time, which prevents registration of electrons of near-equal energy.

large variation with photon energy of the relative intensitites observed for the $^4S$, $^2D$, and $^2P$ states (cf. Table I) reflect a difference of this kind. If this interpretation is correct, the shake-off process seems to favor a statistical distribution and the indirect process primarily transitions to the ground state. More investigations will be made to further explore this aspect.

The only specific calculations of such distributions have been made in the case of Li [13,14], which is unlike the present rare gases in having electrons in two nonequivalent shells. Nevertheless, it is of some interest to compare our results with those calculations. Two one-dimensional distributions are shown in Fig. 6 for triple ionization of Ar at 120 eV with formation of the $Ar^{3+}$ $^2P$ state. As mentioned above, there are indications that this ionization is dominantly direct. Here the excess energy above threshold is 31.5 eV, not too far from the energy excess of 50 eV, where Emmanouilidou [14] has calculated similar distributions for direct triple photoionization of Li. The Ar distributions are flat or slightly U-shaped, like the calculated ones, and show essentially the same shape for two different energies of the third electron.

## IV. SUMMARY

The multiply charged electron-ion coincidence technique is extremely effective in removing both timing uncertainties and unwanted background from multielectron only coincidence measurements on photoionization. The measurements reveal two main mechanisms of triple photoionization, an indirect path via doubly charged intermediate states and a direct three-electron ejection whose characteristics agree in broad outline with predictions of current theory. The lowest state of the triply charged ions is the one most strongly populated by indirect pathways.

## ACKNOWLEDGMENTS

This work has been financially supported by the Swedish Research Council (VR), the Göran Gustafsson Foundation (UU/KTH), the Knut and Alice Wallenberg Foundation, and the Wenner Gren Foundation, Sweden. J.H.D.E. thanks the Leverhulme Trust for financial support. We are particularly grateful to Y. Hikosaka and colleagues for showing us the draft of their paper on triple photoionization of Ar. We are also grateful to the technical support of the workshop staff at the AlbaNova Research Centre in Stockholm as well as at the Ångström laboratory in Uppsala when adopting the experimental setup to synchrotron radiation. Furthermore, we would like to warmly acknowledge the support by the staff and colleagues at BESSY, Berlin. This work was also supported by the European Community–Research Infrastructure Action under the FP6 "Structuring the European Research Area" Program (through the Integrated Infrastructure Initiative "Integrating Activity on Synchroton and Free Electron Laser Science," Contract No. R II 3-CT-2004-506008).

[1] J. S. Briggs and V. Schmidt, J. Phys. B **33**, R1 (2000).
[2] L. Avaldi and A. Huetz, J. Phys. B **38**, S861 (2005).
[3] T. Pattard and J. Burgdörfer, Phys. Rev. A **63**, 020701(R) (2001).
[4] J. Colgan, M. S. Pindzola, and F. Robicheaux, Phys. Rev. Lett. **93**, 053201 (2004).
[5] J. Colgan, M. S. Pindzola, and F. Robicheaux, Phys. Rev. A **72**, 022727 (2005).
[6] A. Emmanouilidou and J. M. Rost, J. Phys. B **39**, L99 (2006).
[7] R. Wehlitz, M. T. Huang, B. D. DePaola, J. C. Levin, I. A. Sellin, T. Nagata, J. W. Cooper, and Y. Azuma, Phys. Rev. Lett. **81**, 1813 (1998).
[8] R. Wehlitz, T. Pattard, M. T. Huang, I. A. Sellin, J. Burgdörfer, and Y. Azuma, Phys. Rev. A **61**, 030704(R) (2000).
[9] A. W. Malcherek, J. M. Rost, and J. S. Briggs, Phys. Rev. A **55**, R3979 (1997).
[10] A. Emmanouilidou and J. M. Rost, J. Phys. B **39**, 4037 (2006).
[11] A. Emmanouilidou and J. M. Rost, Phys. Rev. A **75**, 022712 (2007).
[12] A. Emmanouilidou, P. Wang, and J. M. Rost, Phys. Rev. Lett. **100**, 063002 (2008).
[13] J. Colgan and M. S. Pindzola, J. Phys. B **39**, 1879 (2006).
[14] A. Emmanouilidou, Phys. Rev. A **75**, 042702 (2007).
[15] J. Viefhaus, S. Cvejanovic, B. Langer, T. Lischke, G. Prümper, D. Rolles, A. V. Golovin, A. N. Grum-Grzhimailo, N. M. Kabachnik, and U. Becker, Phys. Rev. Lett. **92**, 083001 (2004).
[16] F. Penent, J. Palaudoux, P. Lablanquie, L. Andric, R. Feifel, and J. H. D. Eland, Phys. Rev. Lett. **95**, 083002 (2005).
[17] P. Lablanquie, L. Andric, J. Palaudoux, U. Becker, M. Braune, J. Viefhaus, J. H. D. Eland, and F. Penent, J. Electron Spectrosc. Relat. Phenom. **156-158**, 51 (2007).
[18] Y. Hikosaka, P. Lablanquie, F. Penent, T. Kaneyasu, E. Shigemasa, R. Feifel, J. H. D. Eland, and K. Ito, Phys. Rev. Lett. (to be published).
[19] P. Kruit and F. H. Read, J. Phys. E **16**, 313 (1983).
[20] J. H. D. Eland, O. Vieuxmaire, T. Kinugawa, P. Lablanquie, R. I. Hall, and F. Penent, Phys. Rev. Lett. **90**, 053003 (2003).
[21] J. H. D. Eland, S. S. W. Ho, and H. L. Worthington, Chem. Phys. **290**, 27 (2003).
[22] J. H. D. Eland, Chem. Phys. **294**, 171 (2003).
[23] J. H. D. Eland, R. Feifel, and D. Edvardsson, J. Phys. Chem. A **108**, 9721 (2004).
[24] A. Pilcher-Clayton and J. H. D. Eland, J. Electron Spectrosc. Relat. Phenom. **142**, 313 (2005).
[25] R. Feifel, J. H. D. Eland, and D. Edvardsson, J. Chem. Phys. **122**, 144308 (2005).
[26] R. Feifel, J. H. D. Eland, L. Storchi, and F. Tarantelli, J. Chem. Phys. **122**, 144309 (2005).
[27] R. D. Molloy, A. Danielsson, L. Karlsson, and J. H. D. Eland, Chem. Phys. **335**, 49 (2007).
[28] P. Linusson, L. Storchi, F. Heijkenskjöld, E. Andersson, M. Elshakre, B. Pfeifer, M. Colombet, J. H. D. Eland, L. Karlsson, J.-E. Rubensson, F. Tarantelli, and R. Feifel, J. Chem. Phys. **129**, 234303 (2008).

[29] A. McPherson, G. Gibson, H. Jara, U. Johann, T. S. Luk, I. A. McIntyre, K. Boyer, and C. K. Rhodes, J. Opt. Soc. Am. B **4**, 595 (1987).
[30] M. Ferray, A. LHuillier, X. F. Li, G. Mainfray, and C. Manus, J. Phys. B **21**, L31 (1988).
[31] Y. Hikosaka, P. Lablanquie, F. Penent, T. Kaneyasu, E. Shigemasa, J. H. D. Eland, T. Aoto, and K. Ito, Phys. Rev. A **76**, 032708 (2007).
[32] D. R. Batchelor, R. Follath, and D. Schmeisser, Nucl. Instrum. Methods Phys. Res. A **467**, 470 (2001).
[33] http://www.bessy.de/
[34] J. H. D. Eland and R. Feifel, Chem. Phys. **327**, 85 (2006).
[35] NIST tables of energy levels of a particular atom or ion, http://physics.nist.gov/PhysRefData/ASD/index.html
[36] C. E. Moore, *Atomic Energy Levels*, Natl. Bur. Stand. (U.S.) Circ. No. 467 (U.S. GPO, Washington, D.C., 1949).
[37] P. Lablanquie, F. Penent, J. Palaudoux, L. Andric, T. Aoto, K. Ito, Y. Hikosaka, R. Feifel, and J. H. D. Eland, in *Photonic, Electronic and Atomic Collisions*, Proceedings of the XXIV International Conference, Rosario, Argentina, 2005, edited by P. D. Fainstein, M. A. P. Lima, J. E. Miraglia, E. C. Montenegro, and R. D. Rivarola (Singapore, World Scientific, 2006), p. 148.